Assessment of Rapid Hepatic Glycogen Synthesis in Humans Using Dynamic ^{13}C Magnetic Resonance Spectroscopy

Stefan Stender [iD] ,[1,2]* Vlad G. Zaha,[3,4]* Craig R. Malloy [iD] ,[3,4] Jessica Sudderth,[5] Ralph J. DeBerardinis,[5] and Jae Mo Park [iD] [3,6,7]

Carbon-13 magnetic resonance spectroscopy (MRS) following oral intake of ^{13}C-labeled glucose is the gold standard for imaging glycogen metabolism in humans. However, the temporal resolution of previous studies has been >13 minutes. Here, we describe a high-sensitivity ^{13}C MRS method for imaging hepatic glycogen synthesis with a temporal resolution of 1 minute or less. Nuclear magnetic resonance spectra were acquired from the liver of 3 healthy volunteers, using a ^{13}C clamshell radiofrequency transmit and paddle-shaped array receive coils in a 3 Tesla magnetic resonance imaging system. Following a 15-minute baseline ^{13}C MRS scan of the liver, [1-^{13}C]-glucose was ingested and ^{13}C MRS data were acquired for an additional 1-3 hours. Dynamic change of the hepatic glycogen synthesis level was analyzed by reconstructing the acquired MRS data with temporal resolutions of 30 seconds to 15 minutes. Plasma levels of ^{13}C-labeled glucose and lactate were measured using gas chromatography–mass spectrometry. While not detected at baseline ^{13}C MRS, [1-^{13}C]-labeled α-glucose and β-glucose and glycogen peaks accumulated rapidly, beginning as early as ~2 minutes after oral administration of [1-^{13}C]-glucose. The [1-^{13}C]-glucose signals peaked at ~5 minutes, whereas [1-^{13}C]-glycogen peaked at ~25 minutes after [1-^{13}C]-glucose ingestion; both signals declined toward baseline levels over the next 1-3 hours. Plasma levels of ^{13}C-glucose and ^{13}C-lactate rose gradually, and approximately 20% of all plasma glucose and 5% of plasma lactate were ^{13}C-labeled by 2 hours after ingestion. *Conclusion:* We observed rapid accumulation of hepatic [1-^{13}C]-glycogen following orally administered [1-^{13}C]-glucose, using a dynamic ^{13}C MRS method with a temporal resolution of 1 minute or less. Commercially available technology allows high temporal resolution studies of glycogen metabolism in the human liver. (*Hepatology Communications* 2020;4:425-433).

Hepatic glycogen is the main buffer for blood glucose levels. Following a meal, hepatocytes take up glucose from the portal vein and store it as glycogen, a branched polymer of glucose residues. Hepatic glycogen content varies 2-fold during the day and can constitute up to 10% of the weight of the liver in humans. During periods of fasting and increased energy demands, hepatic glycogen can be broken down into glucose, which is released into the circulation to maintain blood glucose levels.

Due to its key role in human glucose homeostasis, hepatic glycogen level is an important indicator of the altered hepatic metabolism in a range of metabolic

disorders, including obesity, diabetes, and nonalcoholic fatty liver disease. For example, patients with type 2 diabetes have an impaired rate of glycogen synthesis following a meal, likely due to hepatic insulin resistance and/or an altered insulin to glucagon ratio.[1] Patients with poorly controlled type 1 diabetes can develop glycogenic hepatopathy, a rare disorder characterized by the accumulation of large amounts of hepatic glycogen that ultimately can lead to fibrosis and cirrhosis of the liver.[2] Genetic mutations in enzymes responsible for the synthesis or breakdown of glycogen cause glycogen storage diseases, a family of recessive disorders characterized by an abnormal quantity or quality of glycogen in the liver, muscles, heart, and kidney, depending on the specific molecular defect.

Glycogen metabolism in human patients initially was explored using [3H]- and [14C]-labeled tracers.[3,4] Because of the constraints of radiotracers for clinical research, the gold standard for studying *in vivo* hepatic glycogen metabolism in humans is ^{13}C magnetic resonance spectroscopy (MRS) following oral intake of ^{13}C-labeled glucose. Hepatic glycogen metabolism has been extensively studied using this method in both physiologic and pathologic settings and following intake of various diets and/or drugs. Early studies conducted in the 1980s and 1990s determined the steady-state kinetics of liver glycogen synthesis in fasting and fed healthy individuals.[5,6] Since then, hepatic glycogen metabolism has been studied by MRS in humans with a wide spectrum of traits or diseases, including obesity,[7] type 2 diabetes,[1] and glycogen storage disease.[8]

Due to limited sensitivity, however, these previous MRS-based studies of glycogen metabolism relied on relatively low temporal resolutions, averaging signals of 13 minutes or longer[1,5,9-12]; that is, the earliest time point of hepatic glycogen assessment was 13 minutes after oral intake.[12] The hormonal and neuronal responses to oral food intake are nearly instant. For example, insulin is secreted from the pancreas and glucose is transported from the gut lumen across the enterocytes into the hepatic vein within minutes after glucose ingestion.[11,13] Measuring immediate changes in hepatic glycogen synthesis would therefore require a better temporal resolution than 13 minutes. A fine-scale temporal resolution might provide new insights into the earliest postprandial phase of hepatic metabolism.

Studying the kinetics of hepatic glycogen synthesis during the earliest postprandial period (0-30 minutes) is technically challenging, in part due to the low signal to noise ratio (SNR), which typically requires longer acquisition times and averaging of the signal across many minutes. Alternative methods have been proposed to improve the sensitivity of detecting the glycogen signal. For instance, a novel method for detecting *in vivo* glycogen using water resonance in magnetic resonance imaging (MRI) was recently developed and validated in a mouse model.[14,15] The method has been used in a proof of concept experiment in a recent human study at 3 Tesla (T), but further technological development is required for clinical usage.[16]

Major advances have been made in radiofrequency (RF) technology during the past decades. The SNR has been improved by novel coil designs and by exploiting new MRI techniques, such as parallel imaging.[17] In particular, the recent translation of

ARTICLE INFORMATION:

From the [1]Department of Molecular Genetics, University of Texas Southwestern Medical Center, Dallas, TX; [2]Department of Clinical Biochemistry, Rigshospitalet, Copenhagen, Denmark; [3]Advanced Imaging Research Center, University of Texas Southwestern Medical Center, Dallas, TX; [4]Department of Internal Medicine, University of Texas Southwestern Medical Center, Dallas, TX; [5]Howard Hughes Medical Institute and Children's Medical Center Research Institute, University of Texas Southwestern Medical Center, Dallas, TX; [6]Department of Radiology, University of Texas Southwestern Medical Center, Dallas, TX; [7]Department of Electrical and Computer Engineering, University of Texas at Dallas, Richardson, TX.

ADDRESS CORRESPONDENCE AND REPRINT REQUESTS TO:

Jae Mo Park, Ph.D.
Advanced Imaging Research Center
University of Texas Southwestern Medical Center
5323 Harry Hines Boulevard
Dallas, TX 75390-8568
E-mail: jaemo.park@utsouthwestern.edu
Tel.: +1-214-645-7206

dissolution dynamic nuclear polarization (or hyper-polarization) using ^{13}C-pyruvate accelerated the development of ^{13}C RF coils optimized for imaging various human organs.[18-20] In this study, we hypothesized that a state-of-the-art ^{13}C coil array design (volume carbon transmit coil, designed for hyperpolarized ^{13}C studies) may improve SNR of *in vivo* [13]C glycogen signals. We describe a highly sensitive ^{13}C MRS method that makes it possible to use commercially available technology to observe hepatic glycogen synthesis during the earliest postprandial phase in humans.

Participants and Methods

PARTICIPANTS

We recruited 3 healthy volunteers (38-51 years old, 2 men and 1 woman, all of white European descent). The study was approved by the ethical committee at the University of Texas Southwestern (UTSW) Medical Center. All volunteers provided written consent after having received oral and written information about the study. The participants arrived at the imaging facility at 7 AM after an overnight fast. Before the MRS session, weight and height were measured, blood samples were drawn, and an intravenous access was established.

MRS

We used a system designed for imaging hyperpolarized ^{13}C MRS in human patients: a 3T wide-bore clinical MR scanner (750w Discovery; GE Healthcare), a clamshell ^{13}C transmit coil for RF excitation, and 8-channel ^{13}C receive array paddle-shaped coils for signal reception (dimension of each channel element, 5 × 10 cm; GE Healthcare).[19] Independent studies on a corn-oil phantom (square bottle, 3.78 L) and a ^{13}C-labeled HCO_3^- sphere phantom (1 M; diameter, 40 mm) were performed to determine the sensitivity profile of each coil element. For human studies, ^{1}H images that include three-plane fast gradient-recalled echo and two-dimensional (2D) fast imaging employing steady-state acquisition (FIESTA) (16 slices; breath-hold; echo-time, 1.452 milliseconds; time of repetition [TR], 3.242 milliseconds) were acquired over the liver from each subject, using the GE body coil equipped in the scanner to acquire structural references and to optimize the position of the ^{13}C paddle array coils. Following the ^{1}H scans, a series of pulse-and-acquire ^{13}C MRS scans were performed to monitor metabolism of thermally polarized (not hyperpolarized) [1-^{13}C]-glucose. A baseline ^{13}C MRS liver scan was first performed (TR, 0.5 seconds; flip angle [FA], 60-degree angle; number of scans, 1,800; acquisition time, 15 minutes; spectral width, 10,000 Hz; number of spectral points, 4,096). The ^{13}C MRS scan continued with oral administration of a [1-^{13}C]glucose solution (98 g glucose, containing 20% [1-^{13}C]glucose in 240 mL). Nonslice-selective RF pulse (duration, 512 microseconds) was used for excitation, and the hepatic signal was localized by the paddle coil. ^{13}C MRS scans started concurrently with glucose ingestion and were repeated in 15-minute blocks for up to 3 hours. All free induction decay signals of individual scans were stored for reconstructing the spectra with various temporal resolutions. To confirm the spatial distribution of ^{13}C signals, ^{13}C chemical shift imaging (CSI) (field of view [FOV], 32 × 32 cm; matrix size, 8 × 8; TR, 0.5 seconds; eight averages; slice selective; FA, 60-degree; acquisition time, 4 minutes 16 seconds; spectral width, 10,000 Hz; number of spectral points, 4,096) was performed in participant 2 after MRS scans.

BIOCHEMICAL MEASUREMENTS

Baseline blood samples were analyzed for plasma levels of lipids, lipoproteins, glucose, liver enzyme levels, and markers of kidney function, using standard clinical laboratory methods. Blood samples drawn every 15 minutes during the scan were analyzed for plasma levels of glucose and insulin (by enzyme-linked immunosorbent assay at the Metabolic Phenotyping Core of the UTSW Medical Center) and for ^{13}C-enrichment of glucose and lactate, using gas chromatography–mass spectrometry (GC-MS) at the Metabolomics Facility of the Children's Medical Center Research Institute at the UTSW Medical Center. The GC-MS analysis was performed on the upper phase of a Folch extraction, using 50 μL of plasma. Once dried, the sample was methoximated (10 mg/mL methoxyamine [226904; Sigma] in pyridine [270407; Sigma]) for 15 minutes at 70°C, then derivatized with N-(tert-butyldimethylsilyl)-N-methyltrifluoroacetamide (394882; Sigma) for 1 hour at 70°C. We injected 1 μL of the sample on an Agilent

7890 gas chromatograph coupled to an Agilent 5975 mass selective detector. The detected abundances for the mass isotopomers corresponding to glucose (608-614) and lactate (261-264) were corrected for natural abundance.

DATA ANALYSIS

All the ^{13}C data were processed using MATLAB (Mathworks; Natick, MA). For MRS, the raw data were apodized with a 5-Hz Gaussian filter, zero filled by a factor of 4, and a fast Fourier transform (FFT) applied. The data were analyzed in several temporal resolutions (30 seconds to 15 minutes) by averaging every 60 to 1,800 measurements. After averaging the spectra over time, the zeroth- and first-order phases were corrected in absorption mode. The resulting rolling baseline of the spectra was corrected by fitting to a spline function. Each metabolite was quantified by integrating the peak. For ^{13}C CSI, additional 2D apodization using a hanning filter, 2D zero filling by a factor of 4, and 2D inverse FFT was performed along the spatial domain. ^{13}C metabolite maps were created by integrating the corresponding peaks and overlaid on top of the ^{1}H FIESTA images for display purposes. SNRs of glucose and glycogen were measured from each time-averaged spectrum with 1-minute and 15-minute temporal resolutions by integrating the corresponding peaks. The SNRs are reported for nonoverlapping [1-^{13}C]-glucose (93.3 ppm) and [1-^{13}C]-glycogen (102.2 ppm) peaks only. All data are presented as mean ± SD.

Results

BASELINE CHARACTERISTICS

Baseline characteristics of the 3 volunteers are shown in Table 1. We included 2 men and 1 woman, aged 38, 51, and 46 years, respectively. No volunteer had obesity or diabetes, and all had normal plasma levels of lipids and liver enzymes.

SIGNAL SENSITIVITY OF PADDLE ARRAY COILS

A sensitivity profile of the 8-channel ^{13}C paddle coils, using a bottle container of corn oil and a sphere phantom of 1-M [^{13}C]HCO$_3^-$, is demonstrated in

**TABLE 1. BASELINE CHARACTERISTICS OF THE 3 PARTICIPANTS**

Participant Number	1	2	3
Age (years)	51	38	46
Sex (F/M)	M	M	F
Body mass index (kg/m^2)	28	22	23
Glucose (mg/dL)	92	85	74
Total cholesterol (mg/dL)	305	186	157
HDL cholesterol (mg/dL)	35	60	61
LDL cholesterol (mg/dL)	252	103	81
Triglycerides (mg/dL)	90	113	81
ALT (U/L)	22	30	11

Abbreviations: ALT, alanine aminotransferase; F, female; HDL, high-density lipoprotein, LDL, low-density lipoprotein; M, male.

Fig. 1. Signal sensitivity of each channel decreased markedly with increasing distance to the phantoms. In particular, the sphere phantom signal measured by channel #5-8 was 10%-15% of that measured from channel #2, the channel closest to the phantom. The RF coils were, however, sensitive enough to detect ^{13}C signals located approximately 20 cm away from each coil element.

MRS OF HEPATIC GLYCOGEN SYNTHESIS AFTER ORAL INTAKE OF [1-^{13}C]-LABELED GLUCOSE

While not detected at baseline ^{13}C MRS, [1-^{13}C]-labeled α-glucose and β-glucose (93.3 and 97.2 ppm, respectively) and glycogen (98.5 and 102.2 ppm) peaks accumulated rapidly, beginning as early as ~2 minutes after oral administration of [1-^{13}C]-glucose (Fig. 2). Overall, the dynamic patterns of labeled glucose and glycogen were similar in the 3 participants. When reconstructed with 1-minute temporal resolution, the [1-^{13}C]-glucose signals peaked at 5.3 ± 1.5 minutes, whereas [1-^{13}C]-glycogen peaked at 23.7 ± 1.2 minutes after [1-^{13}C]-glucose ingestion, and both signals declined toward baseline levels over the rest of the MRS session. With 15-minute temporal resolution, however, the glucose and glycogen peaks were at 15 and 30 minutes, respectively. Maximum signal intensity varied somewhat between the 3 participants, likely reflecting differences in body composition and/ or coil placements relative to the liver. The peak SNRs of glucose and glycogen were 76.4 ± 25.6 and 105.1 ± 49.7, respectively, with temporal resolution of 15 minutes, and 26.4 ± 25.6 and 30.3 ± 9.8,
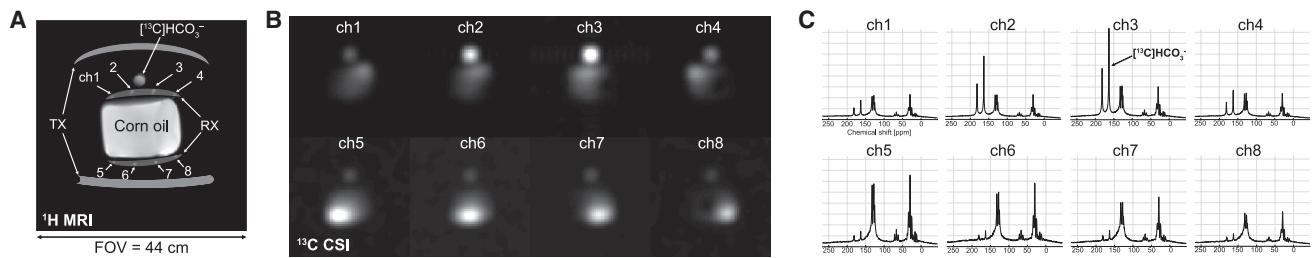
FIG. 1. Sensitivity profile of the RF coils measured using a bottle container of corn oil (1.1% natural abundance of ^{13}C) and a ball phantom of ^{13}C-labeled 1-M HCO_3^-. (A) ^1H MRI showing the positioning of the phantoms relative to the transmit clamshell and 8-channel receive paddle-shaped phased-array ^{13}C RF coils. (B) Coil-wise reconstructed total ^{13}C maps acquired using a free-induction decay chemical shift imaging sequence with a nonselective 90-degree angle RF pulse. (C) Spatially averaged coil-wise magnitude spectra. Abbreviations: ch, channel; RX, receive; TX, transmit.
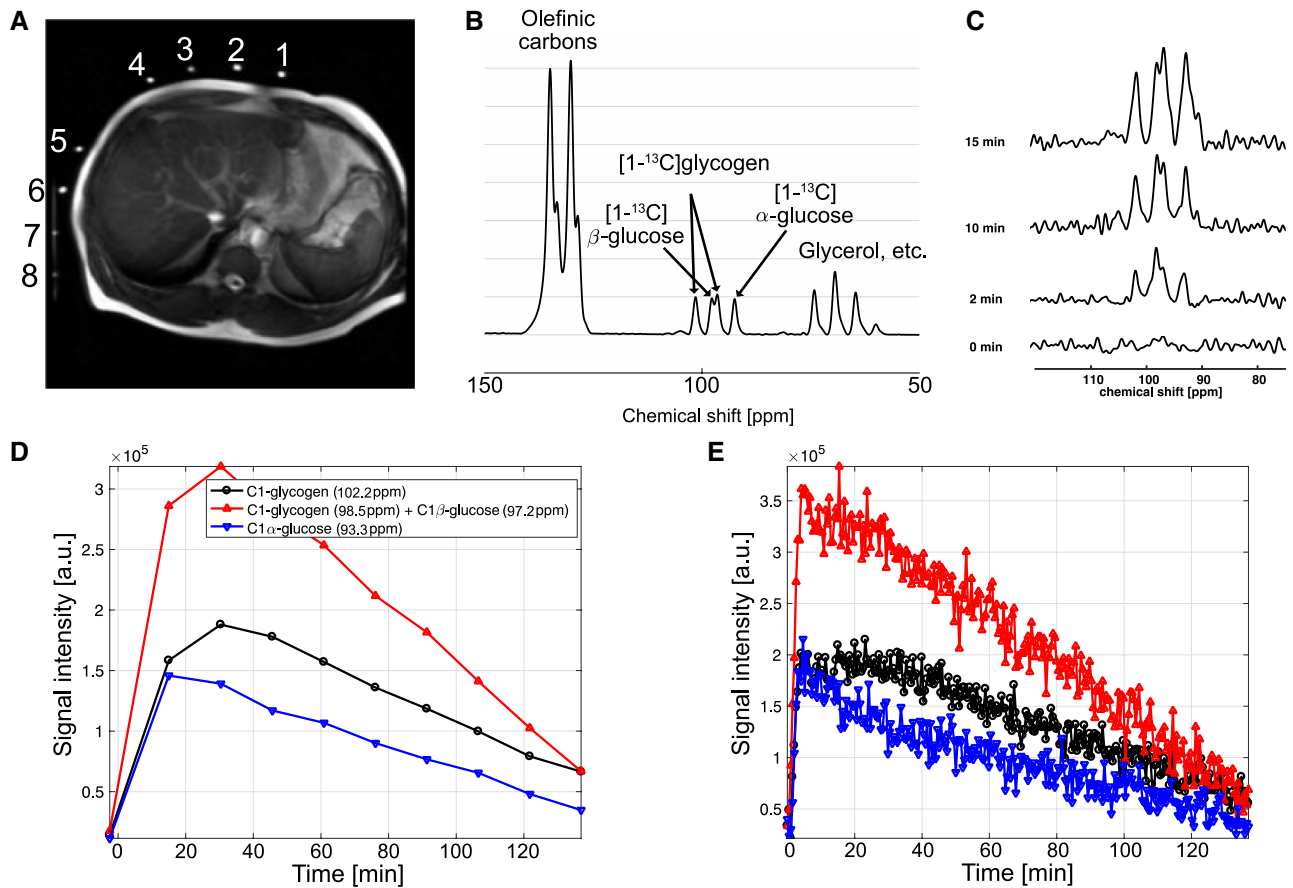
FIG. 2. Real-time hepatic glycogen synthesis of a representative subject (participant 1), measured by dynamic ^{13}C MRS followed by oral administration of [1-^{13}C]-glucose. (A) Axial ^1H MRI showing the position of ^{13}C paddle receive-array coils relative to the liver. Scale = 32 cm by 32 cm. (B) The first 15-minute averaged spectrum following glucose administration and (C) 30-second averaged spectra at 0-, 2-, 10-, and 15-minute time frames showed that glucose and glycogen started to build up rapidly. [1-^{13}C]-labeled glycogen (98.5 and 102.2 ppm) as well as α-glucose (93.3 ppm) and β-glucose (97.2 ppm) could be resolved in each spectrum. Kinetics of [1-^{13}C] α-glucose and β-glucose and [1-^{13}C] glycogen in temporal resolutions of (D) 15 minutes and (E) 30 seconds. Abbreviation: a.u., arbitrary unit.

respectively, with temporal resolution of 1 minute. Depending on the subject, the data could be reconstructed with a finer temporal resolution (<1 minute). Clear ^{13}C-glucose and ^{13}C-glycogen signals from each spectrum when reconstructed every 30 seconds are shown, for example, in Fig. 2 (Supporting Fig. S1).

SPATIAL LOCALIZATION OF [1-^{13}C]-GLYCOGEN PEAKS TO THE LIVER

Although the spatial resolution was limited, separate ^{13}C CSI data confirmed the spatial localization of [1-^{13}C]-glycogen peaks in the liver (Fig. 3). In contrast, [1-^{13}C]-glucose signals were primarily localized in the stomach area. The SNR of [1-^{13}C]-glucose and [1-^{13}C]-glycogen varied among the 3 participants, likely due to the different positioning of the paddle coils relative to the liver. However, glycogen peaks could be resolved even when reconstructed from 30-second-long segments (60 averages; Supporting Fig. S2).

PLASMA LEVELS OF GLUCOSE, LACTATE, AND INSULIN

Following oral ingestion of 98 g glucose (20% [1-^{13}C]-labeled glucose), the fractional ^{13}C enrichment of glucose and lactate rose gradually in the plasma. At 2 hours after ingestion, approximately 20% of all plasma glucose and 5% of plasma lactate were ^{13}C labeled (data from participant 1 are shown in Fig. 4, top panels). Plasma levels of glucose and insulin rose in the 3 participants, reaching peaks at approximately 60 and 90 minutes after intake, respectively, and decreased toward baseline after 60 to 90 minutes (Fig. 4, bottom panels).

Discussion

In this study, we used ^{13}C MRS to observe rapid accumulation of hepatic [1-^{13}C]-glycogen following orally administered [1-^{13}C]-glucose in 3 healthy adults aged 38 to 51 years. In all 3 participants, hepatic glycogen synthesis was detected by ^{13}C MRS as early as 2 minutes after ingestion of labeled glucose. Hepatic glycogen synthesis increased rapidly and peaked at approximately 20 minutes after ingestion. The method uses commercially available technology that may be applied for clinical use. The improved sensitivity of the presented technology to the ^{13}C-labeled glycogen signal allows *in vivo* assessment of dynamic glycogen synthesis every 30 seconds or longer, potentially allowing noninvasive assays and kinetic analysis of the enzymes associated with glycogen metabolism. Many drugs and hormones, such as glucagon and epinephrine, stimulate glycogenolysis with a timeframe of a few seconds. For instance, glucagon stimulates glycogenolysis and gluconeogenesis to raise plasma glucose, but the specific contribution of glycogenolysis versus gluconeogenesis is difficult to determine. Methods that measure glycogen on a minute to minute basis or even faster would allow exploration of such early response mechanisms.
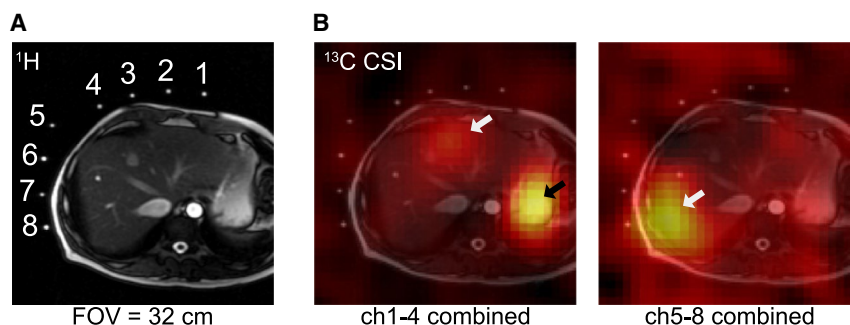
FIG. 3. Spatial distribution of ^{13}C signal after oral administration of [1-^{13}C]-glucose (participant 2). (A) Axial ^{1}H MRI image that shows relative positions of the ^{13}C paddle receive array coils and the slice prescription for ^{13}C CSI. Fiducial markers indicate the location of each channel of the paddle coils. (B) Spatial distribution of the ^{13}C metabolites at 90-110 ppm. The metabolite maps are overlaid over the ^{1}H MRI. [1-^{13}C]-glucose and [1-^{13}C]-glycogen signals are mainly detected from where stomach (black arrow) and liver (white arrows) are located. Signals from the stomach area were dominant in channels #1-4 (B, left), whereas channels #5-8 (B, right) primarily detected signals from the liver. All images scale = 32 cm by 32 cm. Abbreviation: ch, channel.
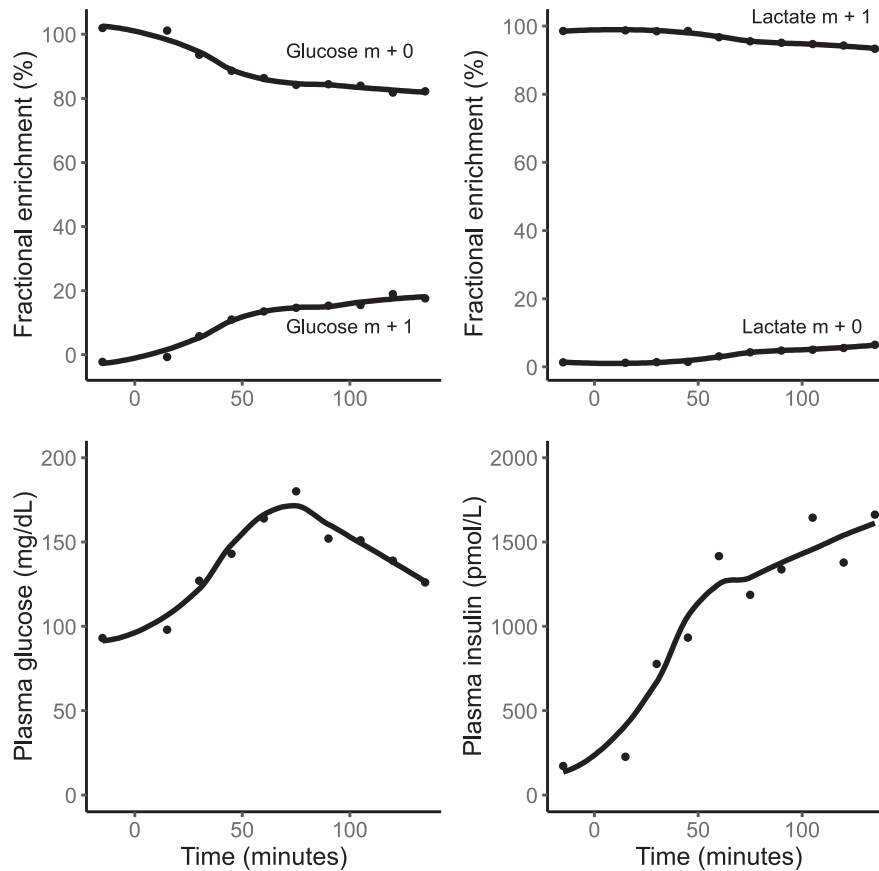
FIG. 4. Temporal trends of plasma ^{13}C-glucose and ^{13}C-lactate and overall plasma levels of glucose and insulin after oral ingestion of [1-^{13}C]-glucose in participant 1. Time of [1-^{13}C]-glucose intake was set as 0. Abbreviation: m, mass.

Early studies have validated the use of nuclear magnetic resonance (NMR) techniques for measurement of ^{13}C metabolic fluxes in animal model systems.[21] The first study that reported natural abundance liver glycogen content in humans used a single 10-cm ^{13}C-only coil and a 2.1T NMR spectrometer.[22] The method was then further refined with the addition of a coplanar ^{1}H-decoupler.[12] The ^{1}H/^{13}C concentric surface coil 11/8 cm configuration reached a time resolution of ~13 minutes and has been used since then in several studies.[1,5,10,23]

In addition to measuring [1-^{13}C]-glucose and [1-^{13}C]-glycogen in the liver using ^{13}C MRS, we used GC-MS to measure ^{13}C-glucose and ^{13}C-lactate in the circulatory system. These plasma measurements provide complementary information on the uptake and metabolism of the ingested bolus of [1-^{13}C]-glucose. Following oral ingestion of ^{13}C-labeled glucose, plasma ^{13}C-glucose would be expected to stem from the following sources: (1) ingested [1-^{13}C]-glucose that is not taken up by the liver and passes directly into circulation after uptake from the intestine, (2) ^{13}C-glucose released from newly synthesized hepatic glycogen (i.e., [1-^{13}C]-glucose that has been taken up by the liver, converted to glycogen, which subsequently undergoes glycogenolysis), and (3) from hepatic gluconeogenesis that used ^{13}C-labeled substrates (e.g., amino acids or lactate) stemming from metabolites of the ingested [1-^{13}C]-glucose bolus. Plasma ^{13}C-lactate would be expected to derive from ^{13}C-glucose taken up and metabolized in red blood cells and muscle cells. We observed that at 2 hours after ingestion, approximately 20% of all plasma glucose and 5% of plasma lactate was ^{13}C labeled. The difference in glucose kinetics between ^{13}C MRS and plasma GC-MS suggests a prompt and effective hepatic uptake of [1-^{13}C]-glucose from the portal vein circulation during the early postprandial period (<30 minutes). Previous studies in animals and humans have estimated the net hepatic glucose uptake following ingestion of an oral glucose

431

load to be between 25% and 40%, depending on the amount of glucose and insulin reaching the liver.[24] Although our study was not designed to assess the metabolic flux of the labeled glucose in detail, it is interesting to note that ^{13}C-glucose and ^{13}C-glycogen accumulated rapidly in the liver at 2 minutes after ingestion, whereas ^{13}C-labeled glucose first appeared in plasma 30 minutes after ingestion. This suggests that the hepatic uptake of orally ingested glucose is close to 100% in the early postprandial phase and that glucose only passes directly into circulation once the hepatic capacity for metabolizing or storing glucose is surpassed. Thus, the presented method may be used to clarify the percentage of glucose passing directly to the circulatory system postprandially.

We also found that hepatic ^{13}C-glycogen decreased after approximately 30 minutes, whereas the fractional enrichment of ^{13}C-glucose in plasma increased from 30 minutes and throughout the remaining scan period. A possible explanation for this pattern is that the participants had been fasting for >12 hours at baseline and were likely relying on glycogenolysis and gluconeogenesis to maintain euglycemia. It is possible that the decreased ^{13}C-glycogen after 30 minutes reflects glycogenolysis of newly synthesized glycogen. We speculate that the last glucose residues incorporated (i.e., those derived from the labeled glucose load) are the first to be released during glycogenolysis. Studies in myofibroblasts support such a "last-in first-out" model of glycogenolysis.[25] It is possible that the pattern would be different in recently fed individuals. We hypothesize that the decrease in ^{13}C-glycogen after 30 minutes would be blunted (or absent) in recently fed individuals after ingestion of labeled glucose compared to the fasting subjects included in our study.

It should be noted that the ^{13}C spectra shown here can be further refined by proton decoupling, which was not available in the MR scanner that we used. For example, the SNR of [1-^{13}C]-glycogen peak can be significantly improved by decoupling the ^{1}H nuclei.[12,26] Moreover, a recent study showed that hepatic mitochondrial oxidative and anaplerotic fluxes can be measured from infused [1-^{13}C]-acetate by measuring [5-^{13}C]- and [1-^{13}C]-glutamate, using ^{1}H-decoupled ^{13}C MRS.[27] Exploiting ^{1}H decoupling, however, requires caution as it increases substantial RF power deposition, which might easily exceed the specific absorption rate limit.

Our study has limitations that should be further investigated. First, we only studied 3 healthy middle-aged adults of white descent and without obesity. The results may therefore not necessarily be generalizable to subjects with different characteristics. For instance, coil placement relative to the liver appeared to majorly influence the sensitivity of the method. It is likely that sensitivity to detect glycogen will be lower in individuals with obesity in whom abdominal fat may hinder placement of the coil in proximity to the liver. Moreover, as the clamshell–paddle coil configuration samples ^{13}C signals from a larger region than coplanar surface coils, the measured spectra likely contain signals from tissue regions other than the liver. In particular, muscle can convert glucose to glycogen under the experimental conditions. However, as the contribution of intracellular and vascular glucose in the liver is minimal, the ^{13}C peaks detected in the liver by the CSI image is primarily glycogen in the liver (Fig. 3, white arrows). Another limitation is that we did not measure absolute levels of hepatic glycogen in our participants. This would have required the inclusion of phantoms with known glycogen concentrations during the scan. We suggest that future studies using the method should include glycogen phantoms, given that the absolute glycogen content of the liver is a biologically as well as clinically relevant measurement.

In conclusion, we observed rapid accumulation of hepatic [1-^{13}C]-glycogen following orally administered [1-^{13}C]-glucose, using a sensitive, high-resolution, time-resolved ^{13}C MRS method. This method, which is based on commercially available and clinically used technology, may be useful for future studies of hepatic glycogen metabolism in humans.

REFERENCES

1) **Krssak M**, **Brehm A**, Bernroider E, Anderwald C, Nowotny P, Dalla Man C, et al. Alterations in postprandial hepatic glycogen metabolism in type 2 diabetes. Diabetes 2004;53:3048-3056.
2) Imtiaz KE, Healy C, Sharif S, Drake I, Awan F, Riley J, et al. Glycogenic hepatopathy in type 1 diabetes: an underrecognized condition. Diabetes Care 2013;36:e6-e7.
3) Clore JN, Post EP, Bailey DJ, Nestler JE, Blackard WG. Evidence for increased liver glycogen in patients with noninsulin-dependent diabetes mellitus after a 3-day fast. J Clin Endocrinol Metab 1992;74:660-666.

4) Clore JN, Blackard WG. Suppression of gluconeogenesis after a 3-day fast does not deplete liver glycogen in patients with NIDDM. Diabetes 1994;43:256-262.

5) Rothman DL, Magnusson I, Katz LD, Shulman RG, Shulman GI. Quantitation of hepatic glycogenolysis and gluconeogenesis in fasting humans with 13C NMR. Science 1991;254:573-576.

6) Shulman GI, Cline G, Schumann WC, Chandramouli V, Kumaran K, Landau BR. Quantitative comparison of pathways of hepatic glycogen repletion in fed and fasted humans. Am J Physiol 1990;259:E335-E341.

7) van der Graaf M, de Haan JH, Smits P, Mulder AH, Heerschap A, Tack CJ. The effect of acute exercise on glycogen synthesis rate in obese subjects studied by 13C MRS. Eur J Appl Physiol 2011;111:275-283.

8) Roser W, Beckmann N, Wiesmann U, Seelig J. Absolute quantification of the hepatic glycogen content in a patient with glycogen storage disease by 13C magnetic resonance spectroscopy. Magn Reson Imaging 1996;14:1217-1220.

9) Petersen KF, Cline GW, Gerard DP, Magnusson I, Rothman DL, Shulman GI. Contribution of net hepatic glycogen synthesis to disposal of an oral glucose load in humans. Metabolism 2001;50:598-601.

10) Taylor R, Magnusson I, Rothman DL, Cline GW, Caumo A, Cobelli C, et al. Direct assessment of liver glycogen storage by 13C nuclear magnetic resonance spectroscopy and regulation of glucose homeostasis after a mixed meal in normal subjects. J Clin Invest 1996;97:126-132.

11) Tura A, Ludvik B, Nolan JJ, Pacini G, Thomaseth K. Insulin and C-peptide secretion and kinetics in humans: direct and model-based measurements during OGTT. Am J Physiol Endocrinol Metab 2001;281:E966-E974.

12) Jue T, Rothman DL, Tavitian BA, Shulman RG. Natural-abundance 13C NMR study of glycogen repletion in human liver and muscle. Proc Natl Acad Sci U S A 1989;86:1439-1442.

13) Shiota M, Moore MC, Galassetti P, Monohan M, Neal DW, Shulman GI, et al. Inclusion of low amounts of fructose with an intraduodenal glucose load markedly reduces postprandial hyperglycemia and hyperinsulinemia in the conscious dog. Diabetes 2002;51:469-478.

14) **van Zijl PC**, **Jones CK**, Ren J, Malloy CR, Sherry AD. MRI detection of glycogen in vivo by using chemical exchange saturation transfer imaging (glycoCEST). Proc Natl Acad Sci U S A 2007;104:4359-4364.

15) Miller CO, Cao J, Chekmenev EY, Damon BM, Cherrington AD, Gore JC. Noninvasive measurements of glycogen in perfused mouse livers using chemical exchange saturation transfer NMR and comparison to (13)C NMR spectroscopy. Anal Chem 2015;87:5824-5830.

16) Deng M, Chen SZ, Yuan J, Chan Q, Zhou J, Wáng YX. Chemical exchange saturation transfer (CEST) MR technique for liver imaging at 3.0 Tesla: an evaluation of different offset number and an after-meal and over-night-fast comparison. Mol Imaging Biol 2016;18:274-282.

17) Fujita H. New horizons in MR technology: RF coil designs and trends. Magn Reson Med Sci 2007;6:29-42.

18) Nelson SJ, Kurhanewicz J, Vigneron DB, Larson PE, Harzstark AL, Ferrone M, et al. Metabolic imaging of patients with prostate cancer using hyperpolarized [1-13C]pyruvate. Sci Transl Med 2013;5:198ra108.

19) Feng Y, Gordon JW, Shin PJ, Von Morze C, Lustig M, Larson PEZ, et al. Development and testing of hyperpolarized (13)C MR calibrationless parallel imaging. J Magn Reson 2016;262:1-7.

20) Chaumeil MM, Ozawa T, Park I, Scott K, James CD, Nelson SJ, et al. Hyperpolarized 13C MR spectroscopic imaging can be used to monitor Everolimus treatment in vivo in an orthotopic rodent model of glioblastoma. Neuroimage 2012;59:193-201.

21) Alger JR, Sillerud LO, Behar KL, Gillies RJ, Shulman RG, Gordon RE, et al. In vivo carbon-13 nuclear magnetic resonance studies of mammals. Science 1981;214:660-662.

22) Jue T, Lohman JA, Ordidge RJ, Shulman RG. Natural abundance 13C NMR spectrum of glycogen in humans. Magn Reson Med 1987;5:377-379.

23) Magnusson I, Rothman DL, Katz LD, Shulman RG, Shulman GI. Increased rate of gluconeogenesis in type II diabetes mellitus. A 13C nuclear magnetic resonance study. J Clin Invest 1992;90:1323-1327.

24) Moore MC, Coate KC, Winnick JJ, An Z, Cherrington AD. Regulation of hepatic glucose uptake and storage in vivo. Adv Nutr 2012;3:286-294.

25) Elsner P, Quistorff B, Hansen GH, Grunnet N. Partly ordered synthesis and degradation of glycogen in cultured rat myotubes. J Biol Chem 2002;277:4831-4838.

26) Beckmann N, Seelig J, Wick H. Analysis of glycogen storage disease by in vivo 13C NMR: comparison of normal volunteers with a patient. Magn Reson Med 1990;16:150-160.

27) **Befroy DE**, **Perry RJ**, Jain N, Dufour S, Cline GW, Trimmer JK, et al. Direct assessment of hepatic mitochondrial oxidative and anaplerotic fluxes in humans using dynamic 13C magnetic resonance spectroscopy. Nat Med 2014;20:98-102.

Author names in bold designate shared co-first authorship.

Supporting Information